Cavitation cloud translation in focused ultrasound

Primary radiation force-mediated effects at varying intensity

Keith Johnston and Paul Prentice*
Institute of Medical Science and Technology (IMSaT)
Division of Imaging and Technology, Ninewells Hospital
University of Dundee, UK
*p.prentice@dundee.ac.uk

Bjoern Gerold
LabTau, INSERM
Université Claude Bernard
Lyon, France

***Abstract*— Cavitation mediated effects in liquids exposed to ultrasound, play pivotal roles in a number of industrial arenas, including precision acoustic cleaning (megasonics) and sonochemistry. The spontaneous occurrence of cavitation, and the subsequent interaction with the liquid and the acoustic field, is however poorly understood, which prevents optimization for any given application. In this paper we report on observations made of single isolated cavitation-bubble clouds, exposed to a well characterized burst of propagating focused ultrasound, and the resulting translational motion of the clouds under the action of the primary acoustic radiation force. As may be expected, larger clouds develop under higher intensity insonations, which translate away from the ultrasound source more rapidly, although a larger associated drag force somewhat tempers the effect. Critically, however, a resonant condition is identified whereby small clouds at lower intensities translate much more rapidly than might otherwise be expected. A model is derived from first principles, adapted to the experimental conditions and demonstrates good agreement with the observations, including the frequency resonance. We anticipate the results will have significance for any application in which understanding and predicting a dynamic cavitating liquid is important, particularly under non-standing wave conditions.**

Keywords—cavitation cloud, focused ultrasound, translation, primary radiation force, resonance

I. INTRODUCTION

Acoustic cavitation – the formation of bubbles in a host medium subject to acoustic radiation – is a dynamic mechanical phenomenon. Strongly driven bubble activity is known to mediate a number of physicochemical effects such as the production or degradation of chemical species (sonochemistry) and the removal of contaminants from a surface, during acoustic cleaning (also known as *megasonics* when ultrasound at frequency of ~1 MHz is used). Despite these applications, cavitation occurrence and and subsequent activity within an acoustic field is generally poorly understood. This is, in large part, due to cavitation being an inherently difficult field of study; bubble dynamics occur on the timescale of the acoustic driving frequency (10's kHz – MHz), with resonant bubbles forming with radii from 100's – a few µms, respectively [1]. Moreover, cavitation occurrence is stochastic, and so the precise moment and location of nucleation is difficult to predict. A compounding factor is that the acoustic field driving the cavitation in a typical observational set-up, is often poorly characterized. Bubble dynamics are known to be highly sensitive to the local acoustic field, including reflections from surfaces and scattered field from other bubbles in the proximity [2]. For example, the primary radiation force in a propagating field will act to translate bubbles in the direction of propagation. If reflections occur and a (partial) standing field results, then sub-resonant bubbles may be expected to conglomerate at pressure antinode positions, with larger than resonant bubbles translating toward node locations. Even this description may be an oversimplification, dependent on the acoustic intensity and bubble sphericity [3]. If other bubbles exist in the locale, then secondary radiative forces can cause strong, and even dominant, inter-bubble attraction and/or repulsion, dependent on the relative bubble size [4].

In this paper, we describe an experimental arrangement that facilitates the observation of cavitation, in response to a well characterized burst of propagating focused ultrasound (Section II). The translation of single isolated cavitation clouds, seeded via the laser-nucleation technique [5, 6] across a range of intensities, is reported (Section III), and compared to a model of the equation of motion for the system (Section IV).

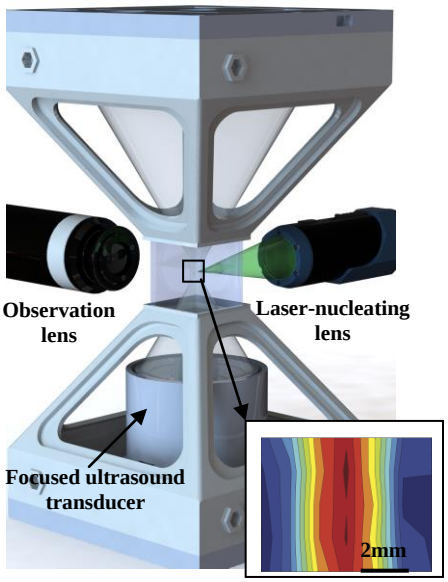

Fig. 1. The sonoptic chamber accommodates the upwardly propagating focused ultrasound field of a transducer, located horizontally, on the base. Cavitation activity is nucleated within a central region, with glass walls for good optical access. Inset: normalized axial scan of acoustic focus, generated *in-situ*.

The research leading to these results has received funding from the European Research Council under the EU FP7 program, ERC grant no. 336189 (TheraCav)

II. Experimental configuration

A. The sonoptic chamber

A sonoptic chamber [6] was custom designed and rapid-prototyped to accommodate the field of a 1.47 MHz focused ultrasound transducer, fabricated in-house. This experimental configuration is specifically designed to permit cavitation observations to be undertaken in a burst of propagating focused ultrasound, without reflection or scatter i.e. no part of the chamber housing perturbs the field, fig. 1. Comprehensive hydrophone scans of the acoustic field at the pressure amplitudes of interest, generated both within the chamber and a $1 \times 1 \times 1$ m^3 scanning tank, confirmed this to be the case. Acoustic absorber material (Precision Acoustics, UK) located at the top of the chamber, minimizes reflection of the primary field, incident from below. For an experiment, the chamber was filled with de-ionised and degassed water (to an O_2 content of below 4 mgL^{-1}), via boiling.

For the results presented, 360 cycles of sinusoid at 1.47 MHz and the voltage required to generate the pre-calibrated peak-negative pressure (PNP) amplitude as quoted, was used to drive cavitation activity. The field at each electronic setting was pre-calibrated with a fibre-optic hydrophone (Precision Acoustics, UK)

B. Laser-nucleation of cavitation

Cavitation is controllably and reproducibly nucleated in a pre-established ultrasound field via a 6-8 ns 532 nm laser-pulse (Litron Lasers, UK) focused with a 50× long working distance objective lens (Mitutoyo, Japan). The pulse energy, measured at the back aperture of the objective lens, was set to 0.9 mJ, which is below the optical breakdown threshold for the host medium. This avoids the large vapor bubbles generally associated with pulsed-laser cavitation studies [7]. The laser-pulse is electronically triggered to arrive at the sonoptic chamber ~70μs following focused ultrasound generation. This ensures ultrasound has both propagated to the central region of the chamber and that the transducer has 'rung-up' to the required PNP value.

C. High-speed imaging

All high-speed data was collected with a Shimadzu HPV-1 (Shimadzu, Japan) camera, imaging at 0.5×10^6 frames per second (fps). This is a single CCD camera capable of recording 100 frames at 312 × 260 pixels. The camera is electronically triggered to capture several frames before the nucleating laser-pulse arrives, to ensure cavitation dynamics are imaged from the outset, and that no pre-existing activity has occurred in the preceding ultrasound exposure. Illumination was achieved through a Xenon flash system (Cordin, USA) coupled to a fibre-optic bundle through a condenser lens. Imaging was undertaken through a 5× 0.14 NA long working distance objective lens (Mitutoyo, Japan), unless otherwise stated.

III. Cloud translation observations

Fig. 2 depicts sample observations of individual cavitation cloud translation at PNPs from 1.1 to 8.9 MPa (± 15%, instrument error, according to manufacturer). Time t = 0 μs is taken as the moment the laser-pulse nucleates activity. The most obvious feature of these sample results is that for higher PNP focused ultrasound, larger clouds form and translate upwards more rapidly, away from the transducer source. The cloud size is due to the degree of fragmentation for the constituent bubbles within the cloud, when they collapse. More energetically driven collapses, under higher intensities, will result in a larger number of secondary bubbles and therefore larger clouds. The translation of the clouds is attributable to the primary radiation force of the focused ultrasound burst, as buoyancy is negligible over the timescale of the imaging. Again, as may be expected intuitively, clouds driven by higher intensity bursts move more rapidly, although the drag force associated with the larger clouds would be expected to limit this effect, as addressed in Section IV. Another interesting feature to fig. 2 is the morphology of the cloud under incrementally increasing PNP. At relatively low pressures (up to 4.6 MPa), the relatively small number of component bubbles retain a quasi-spherical geometry throughout translation. For intermediate PNPs (5.6-6.6 MPa), the sphericity is broken some 30 μs after nucleation, as the cloud adopts an elliptical morphology, elongating along the ultrasound propagation axis. This is perhaps a somewhat surprising observation, as it may have been expected that component bubbles proximal to the transducer might act to 'shield' those distal from radiation force effects. At the highest PNPs (7.8-8.9 MPa), the clouds adopt a distinctive 'mushroom' morphology (arrowed white, fig. 2), reminiscent of those reported previously [8].

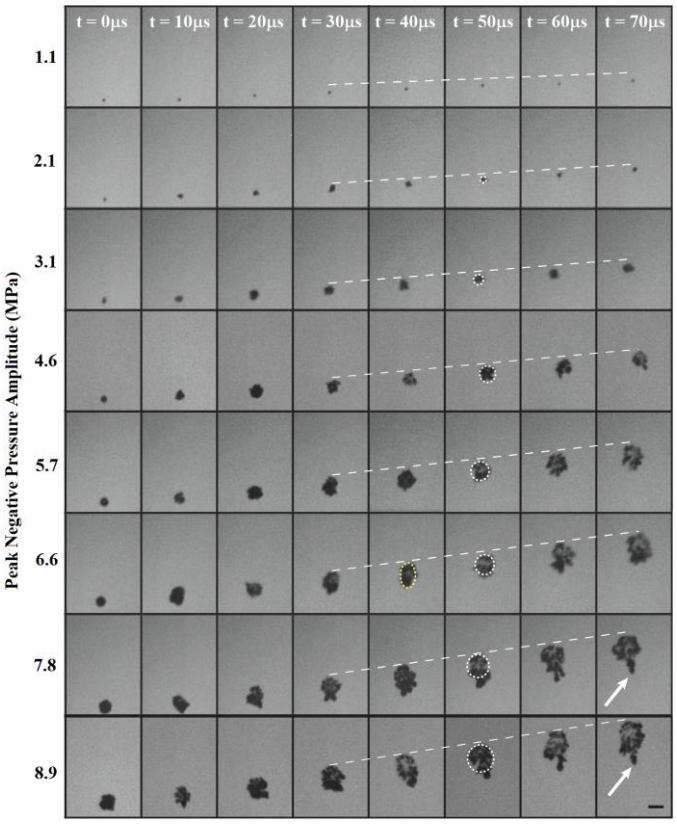

Fig. 2. Representative frames extracted from high-speed image sequences, acquired at 0.5×10^6 fps, of cavitation cloud translation under focused ultrasound bursts of varying PNP, from 1.1 – 8.9 MPa. Scale bar, bottom right: 50μm.

Higher frame-rate observations at higher spatial resolutions would be required to explain the intra-cloud dynamics resulting in the development of such complex morphologies. For comparison to the model outlined in Section IV, an average translational velocity $\bar{v}_t$, is taken as the mean of at least 15 observations of clouds at each PNP, between 30 – 90 µs. As indicated by the dashed white lines of fig. 2, the velocity is approximately constant during this interval, and the longitudinal pressure gradient in this region of the field, $\nabla P_l \sim 0$ (inset, fig.1).

Fig. 3 represents frames from a high-speed sequence recording at PNP = 0.6 MPa. Nucleation of cavitation activity at this pressure amplitude was found to be unreliable, with bubbles forming ~50 % of the time. Moreover, the level of activity was so low that higher spatial resolution observation was required (note different scale bar to fig. 2) and achieved via a 50× 0.42 NA objective lens (Mitutoyo, Japan). When cavitation did occur, it translated much more rapidly than expected from the general trend depicted in fig. 2 (see fig. 5 for overview). It is also notable that the small cloud (or single bubble) is oscillating, with inflation phases arrowed at 6 and 12 µs. The observations recorded at this PNP are an important component to the model and analysis presented in Section IV, and discussed further in Section V.

IV. Equation of Motion and Analysis

The translational velocity of a bubble in a steady fluid subjected to ultrasound can be calculated using eq. 1, [4]

$$F_r + F_d - \frac{d(mv_t)}{dt} = 0 \tag{1}$$

Where F_r is the primary radiation force, F_d the drag force and m the displaced mass of the bubble (cloud), calculated as $m = 2/3\ \pi\rho R_0^3$, where R_0 is the equilibrium radius and ρ the density of the host fluid. Averaging over one acoustic cycle, F_r is given by eq. 2

$$F_r = \frac{(PNP)^2 R_0}{\rho c f_0} \frac{\delta(\frac{f_r}{f_0})}{[(\frac{f_r}{f_0})^2 - 1]^2 + [\delta(\frac{f_r}{f_0})]^2} \tag{2}$$

Where c is the speed of sound in the host fluid, δ is a dimensionless damping coefficient, f_0 is the driving frequency, and f_r resonant bubble frequency [1, 2]. It can be seen from eq. 2 that the radiation force for a bubble of a certain size will be strongly dependent on the acoustic frequency. F_d is given by eq. 3.

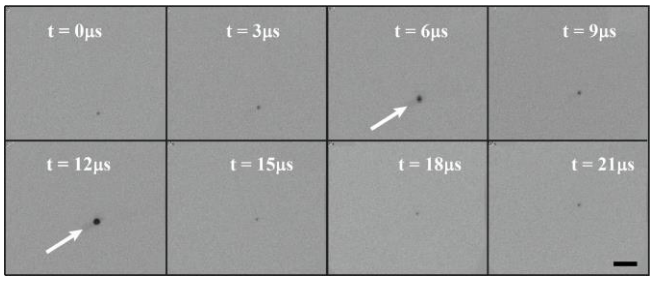

Fig. 3. Minimum level (single bubble or very small cloud) of cavitation activity observed in focused ultrasound of PNP = 0.6 MPa. Inflation phases, indicating oscillatory behavior, arrowed white. Scale bar, bottom right: 20µm.

$$F_d = -\frac{\pi\eta}{4} C_d Re R_0 v_t(t) \tag{3}$$

Where η is the shear (dynamic) viscosity of the fluid, *Re* the Reynolds number, and C_d the drag coefficient. Combining equations (1)-(3), and integrating over time, results in an expression for the translation for the translation speed of a single bubble, in a given ultrasound field, as eq. 4;

$$v_t = \frac{4(PNP)^2}{\rho c f_0 \eta C_d Re} \frac{\delta(\frac{f_r}{f_0})}{[(\frac{f_r}{f_0})^2 - 1]^2 + [\delta(\frac{f_r}{f_0})]^2} [1 - e^{-(\frac{3\eta C_d Re}{8\rho R_0^2} t)}] \tag{4}$$

Which can be simplified according to the experimental parameters as

$$R_0 \ll 1, e^{-(\frac{3\eta C_d RE}{8\rho R_0^2} t)} \to 0 \tag{5}$$

And $C_d Re \sim 24$ [9].

In order to compare this model to the experimental observations, the clouds of figs 2 and 3 are approximated to single bubbles, subject to equivalent acoustic conditions. In terms of the cross-section presented to the primary field, the non-spherical clouds at higher PNPs are further approximated to 'hemispherical heads' as depicted by the white dotted circles of fig 2, at 50 µs. An 'effective cloud radius', R_{eff}, for a given focused ultrasound intensity, was thereby estimated as an average from the high-speed images captured between t = 30 and 90 µs, across the range of PNPs. This empirical data is presented in fig .4. Further adapting eq 4 for the bubble clouds requires that the dependence of R_{eff} on PNP is taken into account. Although R_{eff} is not explicitly used, the corresponding resonant frequency, f_{eff} is inferred from the simplified Minneart equation as $f_{eff} \approx 3/R_{eff}$, [1]. As such, the translational velocity for the cloud is given by eq 6.

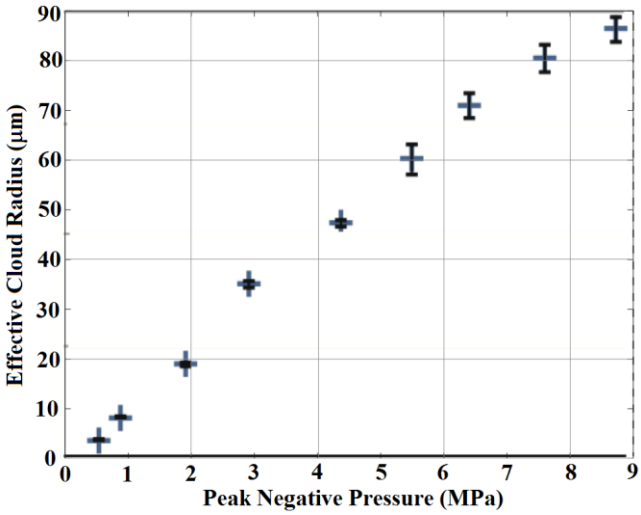

Fig. 4. PNP vs effective cloud radius – experimental data of average radius at each PNP investigated. The error bars depict the standard deviation over n = 15 (n = 6 for 0.6 MPa) observations.

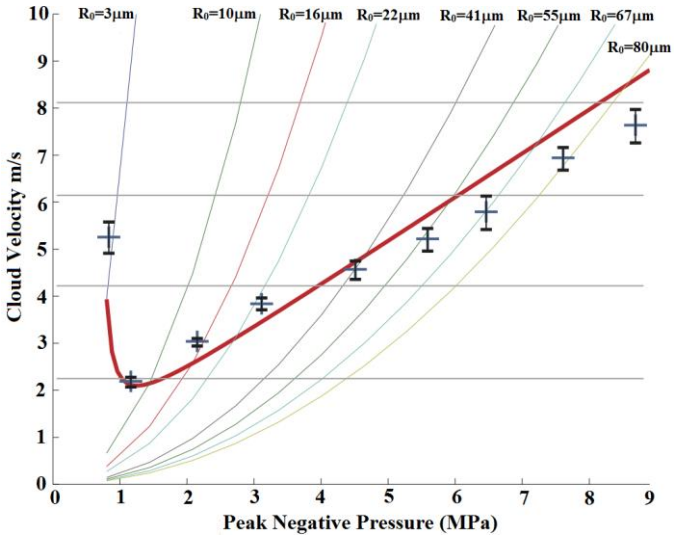

Fig. 5. PNP vs translational velocity, v_t (model), represented by each coloured line, overlaid with $\bar{v}_t$ (experimental) data points using $R_0 = R_{eff}$, the effective cloud radius at a given PNP investigated. The error bars depict the standard deviation over n = 15 (n = 6 for 0.6 MPa) observations The red tick-shaped graph therefore represents the model predictions for comparison to the experimental data.

$$v_t \sim \frac{(PNP)^2}{6\rho c f_0 \eta} \frac{\delta(\frac{f_{eff}(PNP)}{f_0})}{[(\frac{f_{eff}(PNP)}{f_0})^2 - 1]^2} \tag{6}$$

Fig 5 summarizes the results from the model, with experimentally observed cloud translational velocity, $\bar{v}_t$, for the entire data set, and as represented in fig 2 and 3. Each of the colored lines predict how a model single model bubble of the required R_0 (or R_{eff}, dependent on PNP) would translate under the acoustic conditions employed experimentally. The model v_t's for larger R_{eff}'s increase less rapidly with PNP because these (model) single bubbles would be further from the resonant size, determined by the frequency f_0 = 1.47 MHz. The red tick-shaped graph are the model predictions for v_t for single bubbles of R_0 (matching R_{eff} via fig. 4), for the clouds that develop in a given PNP. The data points represent the experimentally obtained cloud $\bar{v}_t$'s, measured from the high-speed sequences, at known PNP.

V. Discussion

The experimental observations demonstrate that cavitation clouds translate, through a water host medium, with velocities in the range of 1 – 10 ms^{-1}, in response to the radiation force of the acoustic field used for this work. Higher PNPs result in more rapid translation, as may be expected, although the larger clouds also result in a more pronounced drag effect, which must be taken into account. A key observation is of the unexpectedly rapid translation for the very small clouds in the lowest PNP investigated of 0.6 MPa, and is accounted for through the identification of a resonance condition for these clouds, in the interaction with the primary field. The volumetric pulsations observed in such cases, represented by fig 3, provide circumstantial evidence in support of this assertion. As the PNP increases, the cloud size also increases above that which is resonant to the field. Accordingly, although the primary radiation force is higher, the cloud translates more slowly. Further increasing the PNP (> 5 MPa) overcomes this 'off-resonance dip' and the translation of the clouds generally increases with radiation force as expected, once drag force is accounted for. The most obvious limitation of the model is the approximation of a cavitation cloud to a single bubble, particularly non-spherical clouds, both in terms of the primary radiation and the drag forces. Despite this, a reasonable agreement with the experimental data is evident. The strong intra-cloud bubble-bubble interaction forces, and the resulting tendency for the cloud to behave as a single entity, as seen in fig 2, despite the strong primary radiation forces at work in the region, would seem to somewhat justify this assumption.

Acknowledgment

We gratefully acknowledge Mr. Adrian Walker of the EPSRC loan pool (UK), for access to the Shimadzu HPV-1 high-speed camera.

References

[1] T. G. Leighton, The Acoustic Bubble. London Academic, 1994.

[2] W. Lauterborn and T. Kurz, "Physics of bubble oscillations" Reports on Progress in Physics, vol 73 106501, 2010.

[3] A. A. Doinikov, "Translational motion of a spherical bubble in an acoustic standing wave of high intensity" Physics of Fluids, vol 14, pp 1420-1425, 2002.

[4] P. Dayton, K. Morgan, A. Klibanov, G. Brandenburger and K. Ferrara, "Optical and acoustical observations of the effects of ultrasound on contrast agents," IEEE Transactions of Ultrasonics Ferroelectrics and Frequency Control, vol 46, pp. 220-232, 1999.

[5] B. Gerold, S. Kotopoulis, C. McDougall, D. McGloin, M. Postema and P. Prentice, "Laser-nucleated acoustic cavitation in focused ultrasound," Review of Scientific Instruments, vol 82, 044902, 2011.

[6] K. Johnston, C. Tapas-Siles, B. Gerold, M. Postema, S. Cochran, A. Cuschieri and P. Prentice, "Periodic shock-emission from acoustically driven cavitation clouds: A source of the subharmonic signal," Ultrasonics, vol 54, pp 2151-2158, 2014.

[7] B. Gerold, P. Glynne-Jones, C. McDougall, D. McGloin, S. Cochran, A. Melzer and P. Prentice, "Directed jetting from collapsing cavities exposed to focused ultrasound," Applied Physics Letters, vol 100, 024104, 2012.

[8] H. Chen, X. Li, M. Wan and S. Wang, "High-speed observation of cavitation bubble cloud structures in the focal region of a 1.2 MHz high-intensity focused ultrasound transducer," Ultrasonics Sonochemistry, vol 14, pp 291-297, 2007.

[9] S. Kotopoulis and M. Postema, "Microfoam formation in a capillary," Ultrasonics, vol 50, pp 260-268, 2010.